GOLF RESULTS: TODAY'S VIEW ON THE SOLAR MODES

G. GREC [2], S. TURCK-CHIÈZE [4], M. LAZREK [7 2]
T. ROCA CORTÉS [3], L. BERTELLO [6], F. BAUDIN [3]
P. BOUMIER [1], J. CHARRA [1], D. FIERRY-FRAILLON [5]
E. FOSSAT [5], A. H. GABRIEL [1], R. A. GARCIA [3 4]
B. GELLY [5], C. GOUIFFES [4], C. RÉGULO [3]
C. RENAUD [2], J.M. ROBILLOT [8], R. K. ULRICH [6]

[1] *Institut d'Astrophysique Spatiale, Unité Mixte CNRS Université Paris XI, 91405 Orsay, France*
[2] *Département Cassini, URA 1362 du CNRS, Observatoire de la Côte d'Azur 06304 Nice, France*
[3] *Instituto de Astrofísica de Canarias, 38205 La Laguna, Tenerife, España*
[4] *Service d'Astrophysique, DSM/DAPNIA, CE Saclay, 91191 Gif-sur-Yvette, France*
[5] *Département d'Astrophysique, URA709 du CNRS, Université de Nice 06034 Nice, France*
[6] *Astronomy Department, University of California, Los Angeles, U.S.A.*
[7] *CNCPRST, 10102 Rabat, Maroc*
[8] *Observatoire de l'Université Bordeaux 1, BP 89, 33270 Floirac, France*

1. Introduction

The SOHO probe was successfully launched on December 2^{nd}, 1995. The performances of the Atlas II flight, the trajectory and the final injection in the Halo orbit around the L1 Lagrangian point left on board a large amount of hydrazine, allowing the possibility for a mission extension later than the 2 planned years. The operations of the GOLF experiment started on January 16^{th} for a period devoted to the initial tests and to the adjustments of the thermal settings. The effective solar observations started on February 18^{th} and are still running. For the studies presented here below, the data set ends

J. Provost and F.-X. Schmider (eds.), Sounding Solar and Stellar Interiors, 91-102.

in mid-September. All tables and figures come from the compilation of the data analysis made in several institutes with different methods, and some complementary or additional results are displayed in the poster booklet published from this symposium.

2. The solar velocity signal

We did use GOLF in nominal mode up to April 1^{st} (A. Gabriel *et al.*, 1995). This mode has been shown to be free from any first order variations and the test conducted for the depointing sensitivity indicates that no perturbing signal is expected from the attitude variations of SOHO. Unfortunately, at the beginning of April, we had to face with mechanical troubles, and due to that, GOLF is no longer used in the nominal differential mode, but is monitoring only the blue resonance windows in the wing of the DI and DII photospheric lines. In these conditions, GOLF data depend at the first order on the seasonal changes of the solar distance, the spacecraft to Sun radial velocity, the solar magnetic activity and also on the possible drifts of the temperature of several instrumental components. Detrending these effects has now become more crucial for the low frequency investigation. In practice, the characteristic time of most drifts is longer than 1 day, so that little real trouble can be confidently expected. On the other hand, the conversion of the photometric signal into velocity is a complex question, because the p-mode oscillations produce other effects than radial velocity changes. This question will be dealt in a future paper. For the study of the p-mode frequencies spectrum, it has been considered of almost no importance and has been addressed as simply as possible.

The data obtained during the time of nominal operation has made possible to compare the solar spectrum obtained for several analyses:

- The "differential photometer mode" analysis, makes use of the successive measurements I_R and I_B in the red or blue wings. The velocity is computed as $V_S = V_0(I_B - I_R)/(I_B + I_R)$, where I_R and I_B are the intensity mesurements for the red and blue channel. V_0 depends on the orbital velocity, but is nearly constant during the February-March run. An approximate value $V_0 = 4000$ m/s comes from laboratory measurements, and a further calibration will come from an analysis of the data versus the orbital velocity.
- The 2 "photometer modes" analyses make use of the fluctuations of either I_R or I_B, converted into velocity signal [1]. Those fluctuations are simply corrected from the photometric sensitivity changes due to the variable distance of the Sun and to the long term thermal drifts, using the low frequency com-

[1]The band-passes are $\simeq$ 35 mÅ, tuned on the wings of the D photospheric lines, and shifted every 5 sec. from $\simeq$ 5 mÅ to monitor the slopes of the lines wings. At this preliminary level of analysis, the information coming from this modulation is not used.

https://doi.org/10.1017/S0074180900061052 Published online by Cambridge University Press

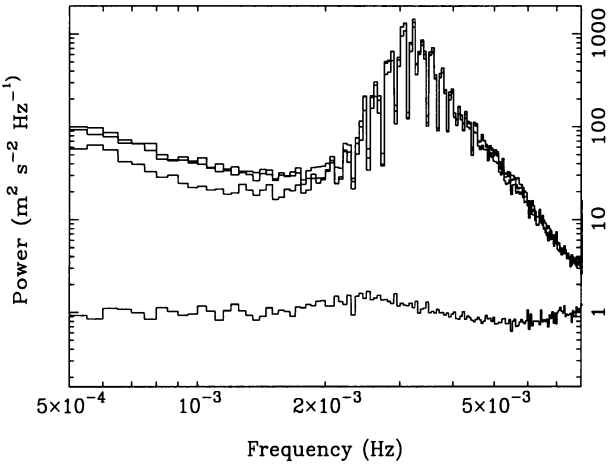

Figure 1. Power spectrum for: velocity in differential mode (the lower of 3 curves), or computed respectively from the blue wing or red wing signals (the 2 upper curves). The noise level in the spectrum below the p-mode frequencies is higher for the 2 "photometer" modes than for the "differential photometer" mode. The curve below displays the ratio V_R/V_B.

ponents of the signal (periods longer than 1 day). This conversion assumes that the measured intensity fluctuations are only sensitive to the weighted sum of the velocity field on the solar disk.

Fig. 1 shows the power spectra obtained after a simulation of the 3 modes with the nominal data set. The 2 "photometer modes" are simply normalized by means of the "differential mode", forcing the integral of the power between 7 and 8 mHz (solar signal, but not p modes) to be the same. This range being close to the Nyquist frequency, the power spectrum folding is avoided by means of a 40 sec sampling of the signal integrated over 80 sec. The 3 spectra contain roughly the same photon noise contribution, they have been smoothed for a better visibility. The increase of power at low frequency (around 1 mHz), where most of the power is expected to be the solar velocity background, can tentatively be interpreted as an increased visibility of the solar granulation. The "photometer mode" using a single wing does not integrate all the solar disk as uniformly as the "differential photometer mode" resulting in a less efficient statistical decrease of the signal due to the granular field. This is true as well for the magnetic activity and supergranules, but remains a small effect.

In the p-mode frequencies range, the ratio V_R/V_B depends on the difference of the photospheric filtering of the modes amplitute, related to the different $\tau = 1$ altitudes for red and blue channel, but also to the contribution of intensity fluctuations in the velocity measurements, which is again an altitude-dependent function.

https://doi.org/10.1017/S0074180900061052 Published online by Cambridge University Press

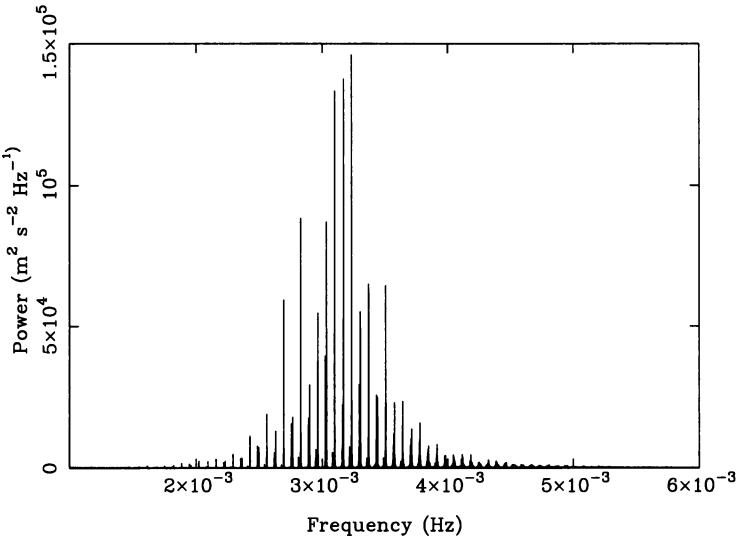

Figure 2. The p-mode power spectrum, showing the low level of noise. The time coverage of the data is practically 100 %.

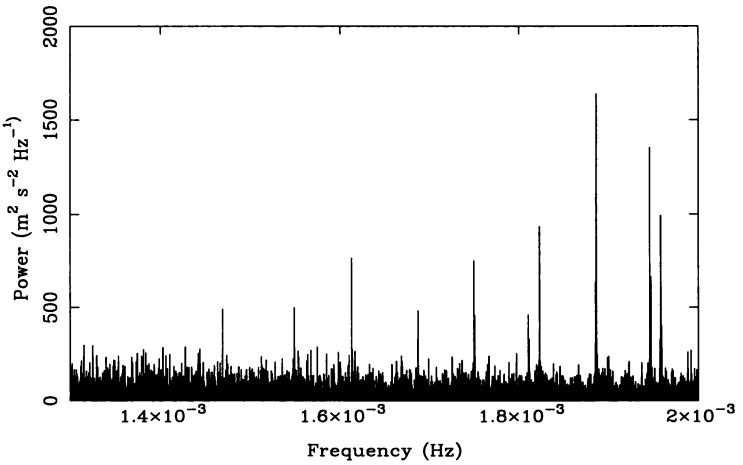

Figure 3. Low frequency part of the p-mode solar spectrum. The amplitude of the lower frequency detected p modes is below 1cm/s.

3. The p-mode analysis

The high resolution power spectrum of the I_B signal measured from April 5^{th} to September 15^{th}, 1996, has been computed with several calibrations techniques. The results are summarized in fig. 2, fig. 3 and fig. 4.

https://doi.org/10.1017/S0074180900061052 Published online by Cambridge University Press

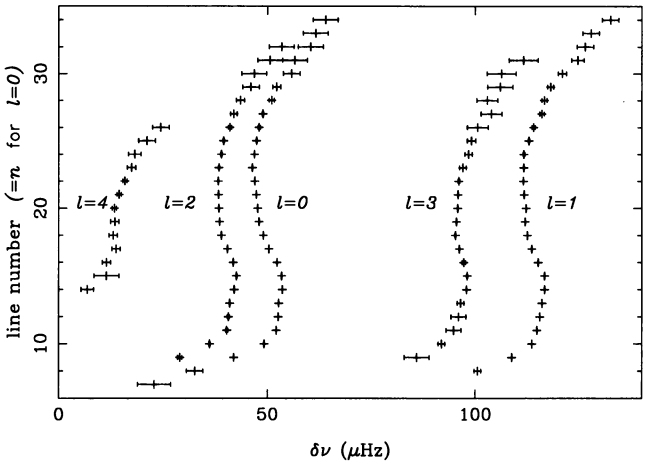

Figure 4. "Echelle" diagram of the p-mode solar spectrum, modulo 135.2 μHz. The frequency ν of a given mode is $\nu = 135.2\ n + \delta\nu + 12$ in μHz. This fig. displays several low amplitude modes not listed in tab. 1.

3.1. *P*-MODE FREQUENCIES

The p-mode parameters are determined by different methods of numerical fit on the velocity power spectrum, including mostly the maximum likelihood fit of Lorentz profiles, singlet or multiplet, according to the degree. In the fit of multiplet, the splitting is assumed to be known (its measurement is another question, explored independently). The estimations of the uncertainty are deduced from a Monte Carlo simulation. Tab. 1 shows the p-mode frequencies and uncertainties (Lazrek *et al.*, 1996-b). The uncertainties are larger than what can be found in former publications. Taking into account only the statistical uncertainty shown by different methods, they are related to the stochastic character of the p modes: less than 6 months of data have been analysed here, and the p-mode temporal behaviour has proved to be a not quite stationary process on the long time scale. A conservative view has been preferred, and in most cases the real error is probably smaller than the listed uncertainty.

3.2. ROTATIONAL SPLITTING

The line profile of a given p mode depends on the excitation and damping processes, but it also shows a multiplet structure due to the solar rotation, called rotational splitting. Note, however, that other physical processes can be invoked as source of rotational splitting, but are not addressed here. Excepted for the lower frequency part of the p-mode spectrum, the separation of the splitted components is of the same order of magnitude as the

https://doi.org/10.1017/S0074180900061052 Published online by Cambridge University Press

TABLE 1. Table of *p*-mode frequencies

n	l=0	l=1	l=2	l=3	l=4
07	1116.64±1.37				
08	1260.52±1.40	1329.22±0.48	1393.21±0.47		
09	1406.72±0.84	1472.65±0.16	1535.37±0.15		
10	1548.38±0.05	1612.78±0.19	1674.50±0.34		
11	1686.60±0.05	1749.23±0.04	1809.92±0.14	1865.07±0.94	
12	1822.21±0.06	1885.08±0.05	1945.71±0.11	2001.23±0.50	
13	1957.44±0.06	2020.85±0.04	2082.14±0.09	2137.96±0.23	
14	2093.55±0.04	2156.79±0.07	2217.97±0.14	2273.11±0.14	2321.28±1.00
15	2228.67±0.07	2291.77±0.08	2352.26±0.08	2407.56±0.42	
16	2362.70±0.08	2425.54±0.08	2485.94±0.11	2541.94±0.21	
17	2495.95±0.07	2559.22±0.07	2619.55±0.08	2676.19±0.30	
18	2629.84±0.07	2693.26±0.06	2754.51±0.06	2811.36±0.10	2864.33±0.45
19	2764.03±0.08	2828.03±0.08	2889.64±0.08	2946.86±0.22	3001.37±0.56
20	2898.80±0.06	2963.50±0.05	3024.75±0.12	3082.27±0.14	3137.78±0.47
21	3033.76±0.04	3098.10±0.08	3159.82±0.09	3217.74±0.15	3273.52±0.54
22	3168.61±0.06	3233.28±0.08	3295.35±0.14	3353.36±0.65	
23	3303.12±0.08	3368.59±0.09	3430.75±0.15	3490.28±0.44	
24	3438.88±0.12	3504.08±0.14	3566.71±0.30	3626.16±0.42	
25	3574.61±0.14	3639.93±0.24	3703.74±0.58	3763.10±2.10	
26	3710.64±0.98	3776.29±0.20	3839.16±1.17	3900.47±1.50	
27	3846.28±0.33	3913.53±0.28	3977.39±0.98	4036.00±2.00	
28	3983.56±0.73	4048.98±0.40	4114.14±1.49	4173.10±3.10	
29	4120.40±0.82	4185.73±0.44	4250.75±1.32	4309.82±3.10	
30	4258.08±1.88	4324.77±0.61	4389.03±1.27		
31	4395.44±1.13	4462.27±0.58			
32	4536.01±2.25	4600.83±1.04			
33	4675.00±3.00				

linewidth, and so its measurement is difficult to achieve with the very high level of accuracy required to invert the rotation deep in the solar sphere. It is mostly a matter of statistics: at the preliminary level of the present analysis, it is not attempted to estimate the splitting for individual modes and global methods have been used to improve the statistics. Those methods have been studied earlier for the analysis of the ground based experiments (Lazrek *et al.*, 1996). Tab. 2 shows the results, averaged over the broadest possible range of radial order for each degree, from l=1 to l=3. Although very preliminary, in term of statistical significance, it can be noticed that, when compared with the ground-based data, the GOLF data show a higher quality level.

https://doi.org/10.1017/S0074180900061052 Published online by Cambridge University Press

TABLE 2. Rotational splitting of p modes

l=1	n=9-21	452 ±14 nHz
l=2	n=10-21	432 ±20 nHz
l=3	n=10-21	449 ±20 nHz

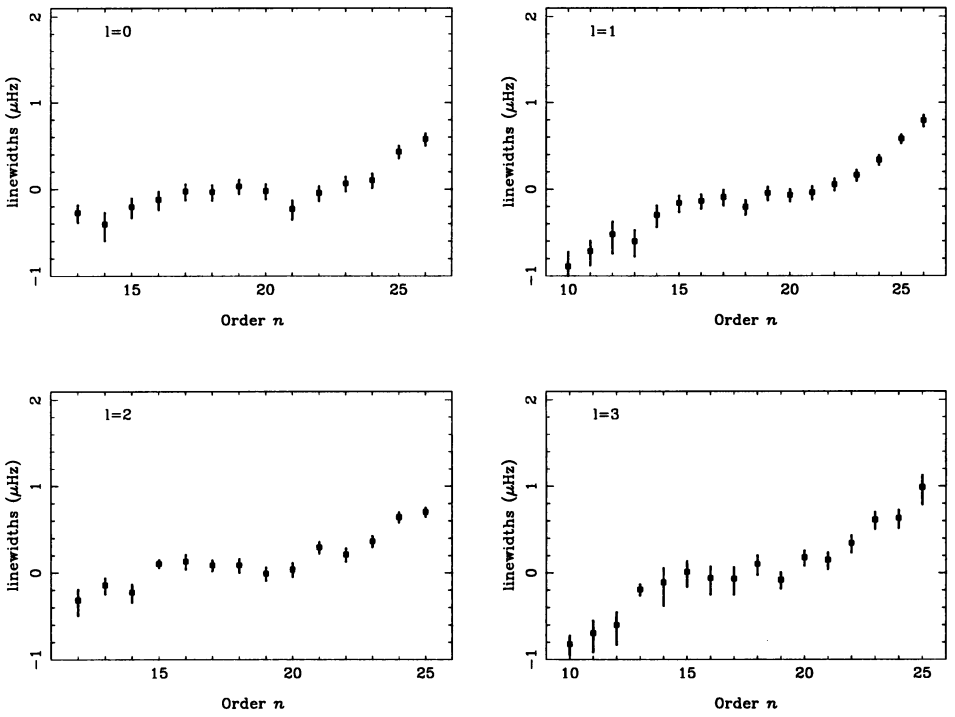

Figure 5. Width of p modes, for degrees $l = 0$ to $l = 3$.

3.3. *P*-MODE LINEWIDTHS

The maximum likelihood fits provide the linewidths, which have been assumed equal for all components of any multiplet. Fig. 5 shows these linewidths for degrees from $l = 0$ to $l = 3$. The general diagonal increase with frequency, as well as the flat or slightly decreasing part in the middle of the p-mode domain, are consistent with the well-known results obtained for intermediate degrees modes (Libbrecht, 1988).

https://doi.org/10.1017/S0074180900061052 Published online by Cambridge University Press

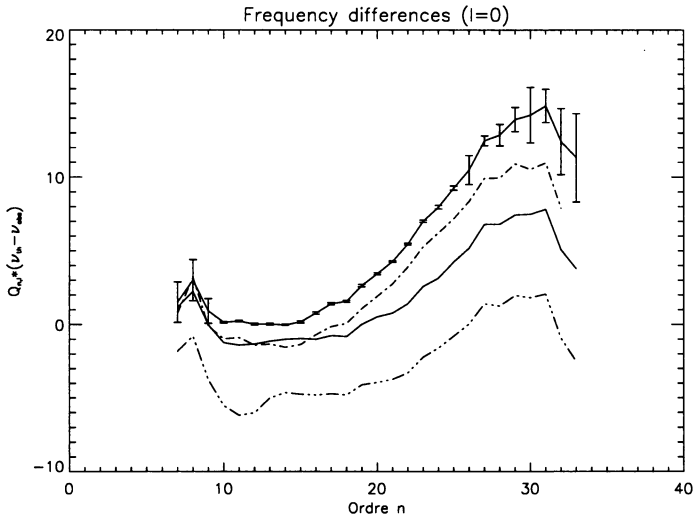

Figure 6. Frequency differences $Q_{n,l} = \nu_c - \nu_o$ for $l = 0$ between the value ν_c computed for solar models coupled with a pulsation code and the acoustic mode frequencies ν_o obtained from the GOLF observations. Full line: Gabriel and Carlier 1996, full line and error bars: Basu *et al.* 1996, −.− line: Guzik *et al.* 1996, −..− line: Turck-Chièze and Lopes 1993 (model without diffusion).

4. Comparison of GOLF acoustic mode frequencies with frequencies deduced from different solar models

Today, 100 acoustic modes penetrating into the region of the solar energy production have been already identified by the GOLF instrument. In order to estimate the information contained in this observation, we first compare the observed frequencies to the ones deduced from different solar models for the radial modes. Fig. 6 shows the difference in absolute values. One notices two general behaviours: the agreement is good for the low values of the radial order for the models including gravitational settling of elements along the solar life, at high frequencies the predictions slightly deviate from the observed values. One may notice that the models for which the slope is reduced, correspond to models which solve the structure equation above the effective radius without introducing a specific atmosphere. This point is illustrated in (Brun *et al.*, 1996) and (Turck-Chièze *et al.*, 1996) which shows that the origin of the discrepancy comes from the description of the very external layers located at ±200 km around the effective radius. In this thin region of the Sun, different processes are in competition, the radiative and convective transport, the turbulent flows and the non adiabatic effects (Kosovishev, 1995), (Guzik *et al.*, 1996). The observed great difference, mainly sensitive to the size of the cavity and the partial ionization of light

https://doi.org/10.1017/S0074180900061052 Published online by Cambridge University Press

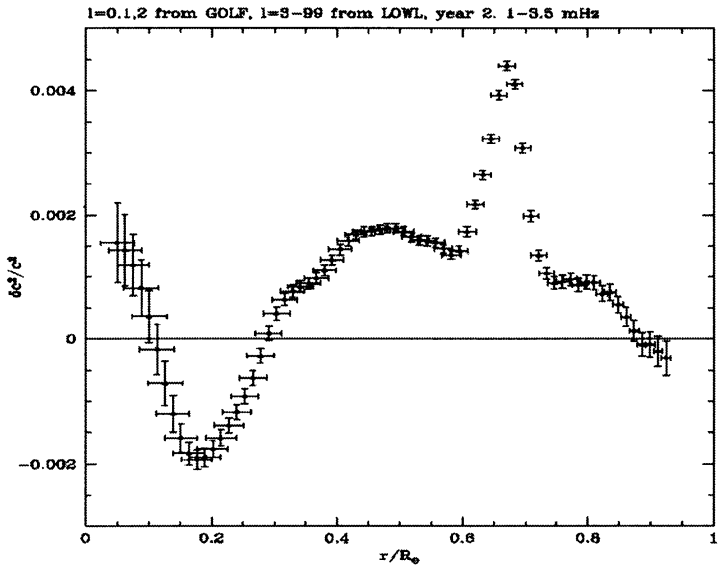

Figure 7. Sound speed difference between the function computed from the acoustic mode frequencies measured with GOLF and LOWL and the recent solar model of Basu *et al.* 1996. Private communication from S. Basu and J. Christensen-Dalsgaard.

elements, together with the observed small difference are well reproduced by the acoustic frequencies deduced from the standard model.

5. Determination of the solar internal sound speed from the GOLF instrument

As far as the nuclear core is concerned, the direct comparison of the frequencies observed and predicted from pulsation models is not very informative and one needs to perform an inversion of the sound speed from the acoustic mode frequencies to better estimate the information obtained by GOLF. The first inversion of the GOLF data (Basu and Christensen-Dalsgaard, 1996) is obtained by coupling these data to the LOWL data set of the second year of measurement from February 95 to February 96 (Tomczyk *et al.*, 1996), which is the most precise and complete list of acoustic mode frequencies presently available. For this inversion, the GOLF list has been limited to the interval from 1.5 mHz to 3.5 mHz, due to the limited available data series for $l > 3$. Fig. 7 shows a precise determination of the sound speed in the solar core. One may notice that the GOLF instrument is able to describe the solar interior with an accuracy in radius better than 0.02 $R\odot$ and a precision on the sound speed better than 0.05 %. We note a good continuity between the GOLF data and the LOWL data in frequency

https://doi.org/10.1017/S0074180900061052 Published online by Cambridge University Press

(Turck-Chièze *et al.*, 1996).
The small deviation from the standard model of about 0.2% in the central core is certainly a great success of solar modelling. Nevertheless, due to the present accuracy of the inversion, this deviation must be confirmed by other solar models and understood in terms of uncertainties on the nuclear reaction rates or other deviations from the standard solar model assumptions. Moreover, the impressive range of acoustic modes presently available encourages some specific investigation to estimate the role of the treatment of the outer layers for the determination of the sound speed in the very central region of the Sun.

6. The Autocorrelation function of the solar oscillations

The spectral resolution of the velocity power spectrum increases obviously with the length of data included, but at the same time the number of fringes in the spectrum seems to increase without limits. This may suggest that the solar oscillations are partially coherent. The autocorrelation function (Fig. 8) of the velocity has been computed on a 70 days data file. The successive maxima of the AC, in the interval $0 < t < 100$ hours are due to the interferences of the p modes, roughly spaced from 68 μHz. For longer delays, the AC reaches a stable value, and this result is consistent with the hypothesis that about 20 % of energy in the p-mode spectrum is due to periodic components (Grec *et al.*, 1996).
To study the statistical life-time of the p modes, we use the more general convolution $B_T(\theta) = V(t) * (V(t)\Pi_T(t))$, where $V(t)$ is the velocity signal and the window $\Pi_T(x) = 1$ for $0 < x < T$ and $\Pi_T(x) = 0$ elsewhere.
Like the AC, the functions $B_T(\theta)$ contain oscillatory components. To compare the amplitudes for several values of T, we extract the absolute value of the envelope of each function, and then filter the result to remove the height frequencies ($\nu_{max} = 1/24h$), this final stage being used to get a readable plot. Fig. 8-b shows the envelope of $B_T(\theta)$ for several values of T. After the initial decrease for $0 < \theta < 100$ h the mean level for each value of T is $\simeq$ proportional to $1/\sqrt{T/15}$, where T is in days. We can then conclude that the p-mode lifetime is close to 15 days, each 15 days time series being independent from each other, value a bit longer than expected from the low frequency p-mode linewidths.

7. The search for g modes

The search for g modes is a major objective of the GOLF experiment. Fig. 9 shows the low frequency part of the velocity spectrum, where a wide number of sharp lines are visible. We need an "Ariane line" to identify the g modes. We made several tests using an asymptotic approximation to

https://doi.org/10.1017/S0074180900061052 Published online by Cambridge University Press

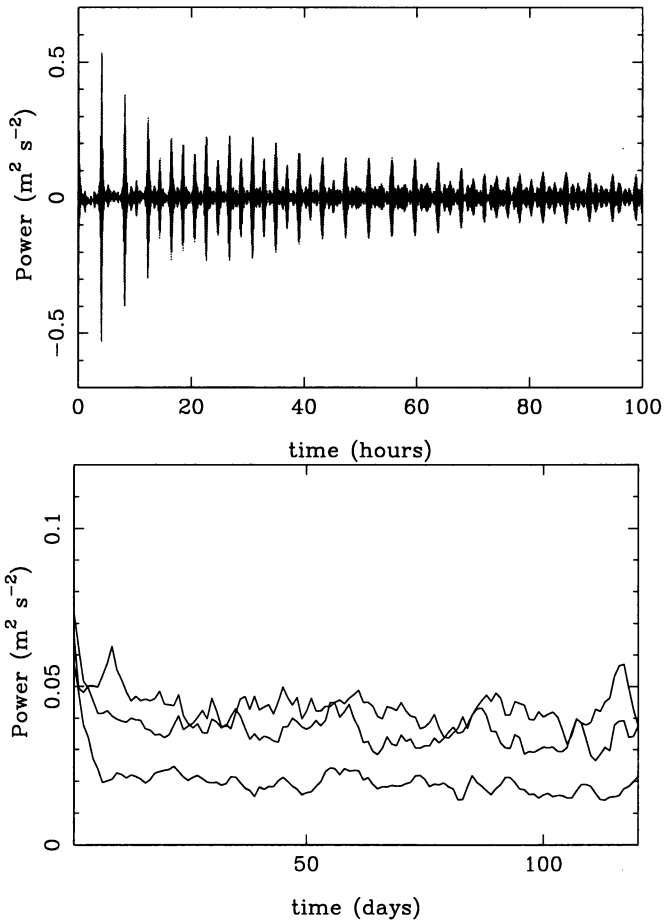

Figure 8. Autocorrelation function of the solar oscillations. Top: the first 100 hours of the AC. Down: the filtered envelope of the amplitude of the B function (see text), from top to bottom for $T = 10$ days,$T = 20$ days,$T = 80$ days.

compute a frequency table (Provost, 1986): changing the model parameters, we can tune the model up to a good correlation level, which may suggest the existence of g modes. Moreover, with the present data, this method seems unable to define a unique set of parameters. A second analysis focuses on the search for modes splitting. No g-mode identification has been achieved. Are the g modes detectable, or even present in the spectrum? The future may give the answers. The analysis of the variations of the instrumental parameters shows no significant signal source at the frequencies observed in the velocity spectrum, in which many low frequency peaks show a long coherence time.

https://doi.org/10.1017/S0074180900061052 Published online by Cambridge University Press

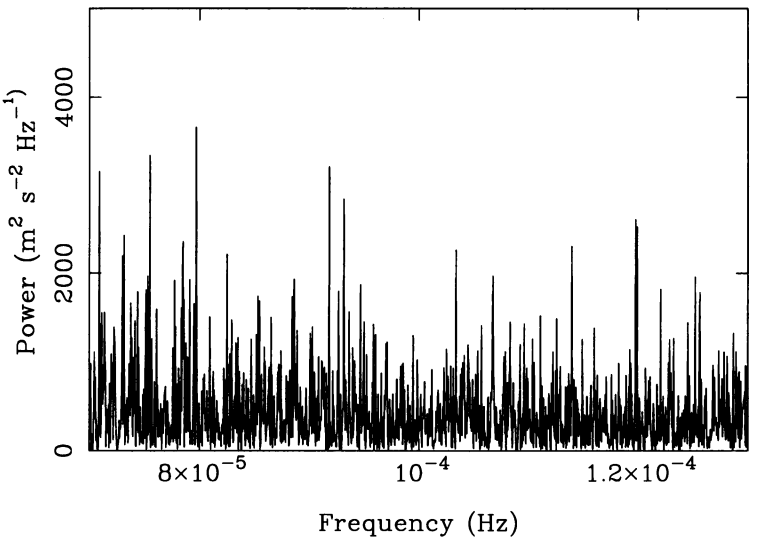

Figure 9. Spectral density in the very low frequency range, next to 100 μHz. The highest amplitudes are below 1 cm/s.

References

Basu, S., Christensen-Dalsgaard J., Schou, J., Thomson, M. J., Tomczyk, S. (1996) *Bull. of Astron. Soc. of India* **24-2**, p. 147.

Basu, S. & Christensen-Dalsgaard J. (1996) private communication.

Brun, S., Lopes, I., Morel, P., Turck-Chièze S. (1996) poster, this conference.

Gabriel A.H., Grec G., Charra J., Robillot J.M., Roca Cortés T., Turck-Chièze S., Bocchia R., Boumier P., Cantin E., Cespédes E., Cougrand B., Crétolle J., Damé L., Decaudin M., Delache P., Denis N., Duc R., Dziko H., Fossat E., Fourmond J.J., Garcia R.A., Gough D., Grivel C., Herreros J.M., Lagardère H., Moalic J.P., Pallé P.L., Pétrou N., Sanchez M., Ulrich R.K., van der Raay H.B. (1995) *Sol. Phys.* **162**, p. 61.

Gabriel, M. & Carlier, F. (1996) *Astron. Astrophys.* to appear.

Grec G., Gabriel M., Renaud C. & the GOLF team (1996) poster, this conference.

Guzik, J., Cox, A.N., Swenson, F.J. (1996) *Bull. of Astron. Soc. of India* **24-2**, p. 161.

Kosovishev, S. (1995) *Fourth SOHO workshop* ESA SP-376 vol. 1, p. 165.

Lazrek, M., Pantel, A., Fossat, E., Gelly, B., Schmider, F.X., Fierry-Fraillon, D., Grec, G., Loudagh, S., Ehgamberdiev, S., Khamitov, I., Hoeksema, T., Pallé, P.L., Régulo, C. (1996) *Sol. Phys.* **166-1**, p. 1.

Lazrek M., Régulo C. R., Baudin F., Bertello L., Garcia R. A., Gouiffes C., Grec G., Roca Cortès T., Turck-Chièze S., Ulrich R. K., Robillot J. M., Gabriel A. H., Boumier P., Charra J. & the GOLF team (1996) poster, this conference.

Libbrecht, K.G. (1988) ESA SP 286, p. 3.

Provost, J. & Berthomieu, G. (1986) *Astron. Astrophys.* **165**, p. 218.

Tomczyk, S., Streander, K., Card, G., Elmore, D., Hull, H., Cacciani, A. (1995) *Sol. Phys.* **159-1**, p. 1.

Turck-Chièze, S. & Lopes, I. (1993) *Astrophys. J.* **408-1** , p. 347.

Turck-Chièze S., Basu, S. Brun S., Christensen-Dalsgaard J., Eff-Darwich A., Gabriel M., Henney C. J., Kosovichev A., Lopes I., Paternò L., Provost J., Ulrich R. K. & the GOLF team (1996) poster, this conference.